RSC Advances

ROYAL SOCIETY OF CHEMISTRY

www.rsc.org/advances

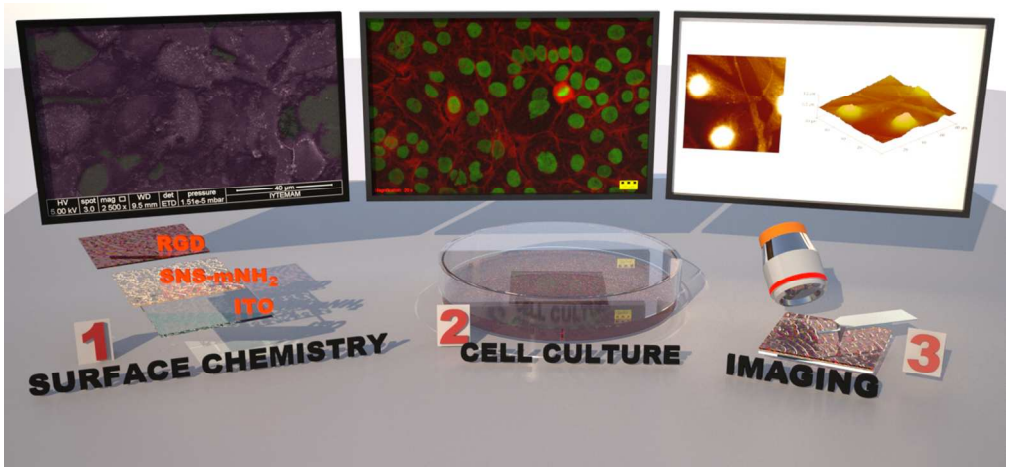

464x214mm (72 x 72 DPI)

Peptide Modified Conducting Polymer as Biofunctional Surface: Monitoring of Cell Adhesion and Proliferation

G. Oyman, C. Geyik, R. Ayranci, M. Ak, D. Odaci Demirkol, S. Timur, and H. Coskunol

Table of Contents

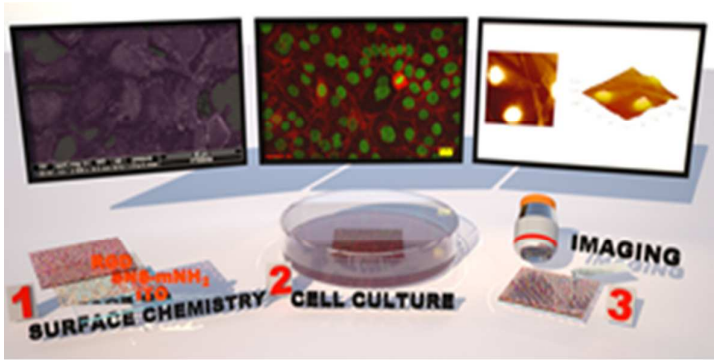

Designed bio-functional surface is a promising candidate for *cell-culture-on chip* applications.

Journal Name

RSCPublishing

ARTICLE

Peptide Modified Conducting Polymer as Biofunctional Surface: Monitoring of Cell Adhesion and Proliferation

Cite this: DOI: 10.1039/xoxxoooooox

Received ooth January 2012,
Accepted ooth January 2012

DOI: 10.1039/xoxxoooooox

www.rsc.org/

Gizem Oyman[a], Caner Geyik[b], Rukiye Ayranci[c], Metin Ak[c], Dilek Odaci Demirkol[b,d*], Suna Timur[b,d*] and Hakan Coskunol[b,e]

Here we report the electropolymerization of 3-(2,5-di(thiophen-2-yl)-1H-pyrrol-1-yl)aniline monomer on ITO glass and its use as a coating material for the cell culture applications. Functional amino groups on the conducting polymer provide post-modification of the surface with arginylglycylaspartic acid (RGD) peptide via EDC Chemistry.
Scanning electron microscopy, atomic force microscopy, contact angle and surface conductivity measurements were carried out for the surface characterization. The peptide conjugated surface was applied for adhesion and proliferation of several cell lines such as Monkey kidney epithelial (Vero), human neuroblastoma (SH-SY5Y), and human immortalized skin keratinocyte (HaCaT). These cells were cultured on RGD modified-, polymer coated-ITO glass as well as conventional polystyrene surfaces for the comparison. Data indicate that, the RGD modified surfaces exhibited better cell adhesion and proliferation among all surfaces compared. Cell imaging studies up to 72 h were performed on these surfaces by different microscopy techniques. Therefore, the novel bio-functional substrate is a promising candidate for further studies such as monitoring the effects of drugs and chemicals on the cellular viability and morphology as well as *cell-culture-on chip* applications.

Introduction

The mechanisms of life and their effects to diseases form the basis of biological researches. Due to the dynamic nature of the biological organizations, monitoring of living cells and the effects of drugs and chemicals on mammalian cells has essential importance. In recent years, *lab-on-a chip* systems have been introduced to detect cellular organizations quickly and accurately. These systems have many different advantages such as miniaturization, increased sensitivity, having opportunity for high throughput screening, and reduced cost.[1] Because the *lab-on-a chip* is a reliable candidate for monitoring living cells, enormous amount of research has been conducted for designing functional surfaces with increased sensitivity.[2, 3]
Polymers have been preferred for many years, owing to their modification capabilities with different side groups. Examples of polymers used as surface materials include polystyrene, polypyrole, polyaniline, and polythiophen.[4-6] Particularly, conducting polymers are promising materials for tissue engineering and electrochemical-based bioanalytical systems due to their alterable physical, chemical and electrical properties.[7, 8] Especially, electrochemically deposited polymers are advantageous because of controllable thickness and morphological properties by changing applied voltage or current.[9-13] Up to now, a number of strategies have been developed to obtain an increased biocompatibility of conducting polymers. One of them is to modify these polymers with several bioactive molecules such as enzymes, nucleic acids, polypeptides, and antibodies in order to increase biocompatibility and selectivity.[14-19]
Cell adhesion, which occurs before various events for anchorage-dependent cells such as cell proliferation, cell migration and differentiated cellular function, is very important step for microarray platforms, development of miniaturized bioanalytical systems, and cell-substrate platforms for tissue engineering applications.[20, 21] Cell adhesion is affected directly from surface hardness, topographical properties and electrical charge of biomaterials.[22-24] Researchers have developed numerous surfaces to investigate cell adhesion, which have different properties.[25-27] Surfaces coated with extracellular matrix (ECM) proteins, such as positively charged poly-L-lysine, fibronectin, collagen and laminin, have widespread usage due to their cell adhesive properties.[28-30] Although ECM proteins increase cell adhesion on surfaces, they have several disadvantages such as uncontrolled thickness, containing different cell recognition motifs, and being object to proteolytic degradation.[31-33] Therefore, it is so important to design surfaces

with controlled thickness and suitable distribution of the bioactive molecules for cell adhesion. RGD (R: Arginine, G: Glycine and D: Aspartic acid) is a frequently used tripeptide as a cell adhesion motif.[31] It is advantageous to use RGD instead of ECM proteins owing to its controlled orientation on surfaces. Additionally, it is stable molecule against sterilization processes, denaturation and enzymatic degradation.[34]

In this work, a monomer; 3-(2,5-di(thiophen-2-yl)-1H-pyrrol-1-yl)aniline (SNS-mNH$_2$) was synthesized according to the similar procedure in the literature.[35] The corresponding monomer structure has a great advantage due to its amino group which is open to amide bonding. Also, the thiophenepyrrole-thiophene polymerize easily. Indium Tin Oxide (ITO) coated glass was used as working electrode. ITO-glass is most advantageous for light microscopy techniques due to its transparent nature. Modified ITO surfaces can be combined with PDMS and such polymers to create cell culture chambers for *lab-on-a-chip* systems.[1, 36-40] The conducting polymer SNS-mNH$_2$ was electrochemically deposited onto ITO-glass by cyclic voltammetry (CV) technique. In order to provide cell adhesion on the modified surfaces, RGD peptide was used. Poly-(SNS-mNH$_2$) served as an excellent immobilization matrix. Introduction of RGD onto the polymer coated surface was performed through covalent binding using the well-established two-step carbodiimide coupling method.[41] Surface properties and morphology were analyzed by contact angle measurement, scanning electron microscopy (SEM) and atomic force microscopy (AFM). African green monkey kidney (Vero), human keratinocyte (HaCaT) and human neuroblastoma (SH-SY5Y) cell lines were cultivated and monitored by fluorescence microscopy (FM) to test cell adhesion and proliferation on modified surfaces. Also, cell morphology on modified surfaces was examined by SEM and AFM.

Results and discussion

Synthesis of 3-(2,5-di(thiophen-2-yl)-1H-pyrrol-1-yl)aniline

Structure of the SNS-mNH$_2$ was characterized ^{1}H-NMR and ^{13}C-NMR spectra. Characteristic peaks for SNS-mNH$_2$ in ^{13}C-NMR spectroscopy (Fig. S1) are listed below: ^{13}C NMR (400 MHz, $CDCl_3$) δ: 191.46, 143.77, 133.74, 132.18, 129.94, 128.20, 126.97, 123.79, 120.11, 116.43, 115.70, and 109.48. In the ^{1}H-NMR the zero chemical shifts was assigned to TMS. Characteristic peaks for SNS-mNH$_2$ in ^{1}H-NMR spectroscopy (Fig. 1) are listed below: $C_{18}H_{14}N_2S_2$, δH ($CDCl_3$): 3.68 (s, 2H, H_a), 6.44 (dd, 2H, H_b), 6.53 (m, 2H, H_c), 6.74 (dd, 2H, H_d), 6.97 (dd, 2H, H_e), 7.07 (m, 2H, H_f), 7.57 (dd, 2H, H_g), 7.74 (dd, 2H, H_h).

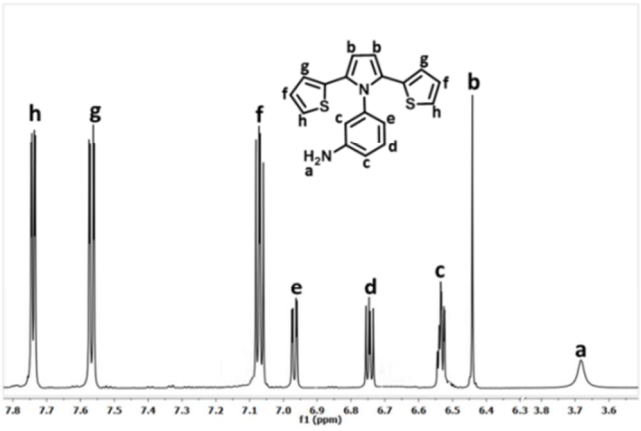

Fig. 1. ^{1}H-NMR spectra of SNS-mNH$_2$ monomer.

Electrochemical polymerization of the monomer

Poly-(SNS-mNH$_2$) film was prepared via potentiodynamic electrochemical polymerization. In the first cycle of the cyclic voltammogram of polymer (Fig. 2), the monomer is oxidized to its radical cation at +0.84 V. Monomer oxidation is immediately followed by chemical coupling that yields oligomers in the vicinity of the electrode. Once these oligomers reach a certain length they precipitate onto the ITO-glass where the chains can continue to grow in length [42]. It can be monitored by the appearance of a peak (+0.36 V) corresponding to the reduction of the oxidized polymer while scanning in the cathodic direction. A second positive scan reveals another oxidation peak (+0.52 V) at a lower potential than the monomer oxidation peak, which is due to the oxidized polymer. Another noticeable fact is the increase in monomer oxidation peak current in the subsequent scans. As the peak current is directly proportional to the electrode area, this increase in the peak current may be attributed to an increase in the area due to the electrodeposited polymer. [43]

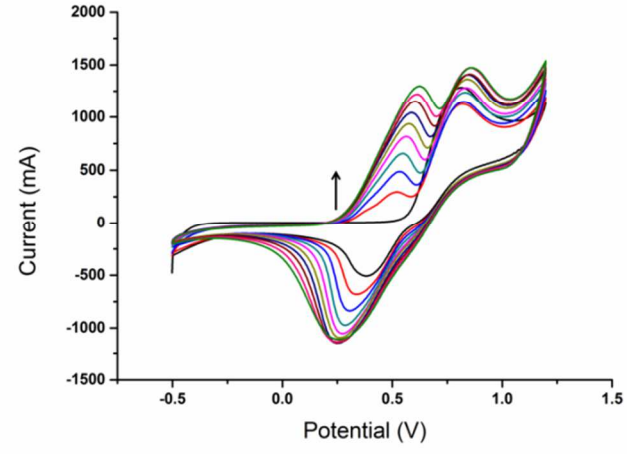

Fig. 2. Repeated potential-scan electropolymerization of SNS-mNH$_2$ monomer in 0.1 M $NaClO_4$/$LiClO_4$/Acetonitrile electrolyte/solvent system at a scan rate of 100 mV s^{-1} on ITO-glass (up to 10 cycles).

Modified surface characterization

Fig. S2 shows CV of poly-(SNS-mNH$_2$) at different scan rates. The current responses were directly proportional to the scan rate indicating that the polymer films were electroactive and well adhered to the surface. The scan rates for the anodic and cathodic peak currents show a linear dependence as a function of the scan rate in the range from 25 to 250 mV/s (Fig. S2 inset). This demonstrates that the electrochemical processes are not diffusion limited and reversible even at very high scan rates. Surface modification impacts on the electrochemical signal transduction were investigated by differential pulse voltammetry (DPV) which gives detailed information about redox characteristics of chemicals. DPV of bare ITO (ITO), polymer coated ITO (ITO/SNS-mNH$_2$) and RGD modified ITO (ITO/SNS-mNH$_2$/RGD) surfaces were performed between +0.5 V and -0.3 V. A decrease in the peak current values was observed for SNS-mNH$_2$-deposited (-0.179 mA; ΔE_{Pc} = +0.24 V) and RGD modified surfaces (-0.065 mA; ΔE_{Pc} = +0.25 V) when compared to bare ITO (-0.359 mA; ΔE_{Pc} = +0.20 V) (Fig. 3). This might be due to the increased thickness of electroactive surface possible diffusion layers on the surface.

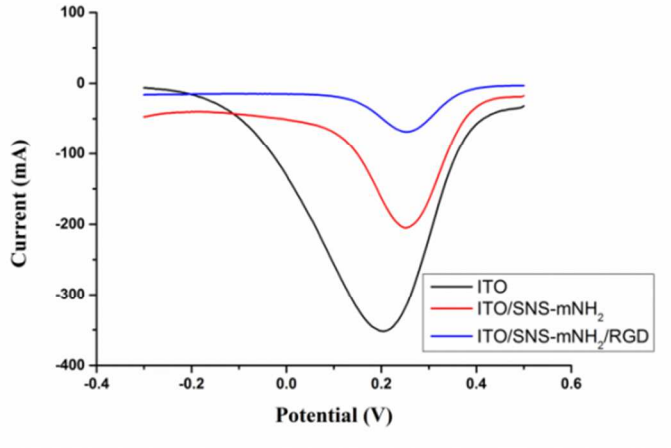

Fig. 3. Differential pulse voltammetry results of ITO (Blue), ITO/mSNS-NH$_2$ (Red) and ITO/SNS-mNH$_2$/RGD (Black) in 5.0 mM [Fe(CN)$_6^{3-/4-}$] at a scan rate of 50 mVs^1 (n=3).

Two probe measurements were performed to gain information on the changes of electrical conductivity of the surfaces before and after modification with the peptide sequence. Two methods are commonly employed for the measurement of conductivity of conducting materials. These have been referred to as 2-probe and 4-probe methods. For semiconductors and insulators where resistivity of sample itself is very high, the contact resistance becomes negligible; 2-probe method is applicable. The electrical conductivities of the samples have been obtained from surface resistance measurements by 2-probe method as their resistances are relatively high. The conductivity of modified surfaces were determined to be 3.0 x10^3, 1.0 x 10^3 and 0.9 x 10^3 (Ω cm)$^{-1}$ for ITO, ITO/SNS-mNH$_2$, and ITO/SNS-mNH$_2$/RGD, respectively. According to the results, there is a decrease in the conductivity of the surfaces after each modification steps. However, conductivity of the surfaces maintained. The ultimate surface has substantially high conductive properties when compared to similar conducting polymers.[44, 45] Thus, it is possible to use proposed surface in platforms that is conductive and biofunctionalized to improve cell adhesion. In order to gain information on the changes of hydrophilicity of the surfaces before and after conjugation with the RGD peptide, contact angle measurements were performed. A drop in the advancing angle from 83.6° ± 1.1° to 78.9° ± 0.9° was observed after RGD immobilization on the –NH$_2$ functional surface (n=5 and p = 0.0079).

Surface morphologies before and after biomolecule immobilizations were examined by SEM. According to the Fig. 4a and 4b, conducting polymer was grown homogeneously on the ITO glass. On the other hand, the surface morphology of the RGD modified surface (Fig. 4c) depicts a rough coating on the surface. This clearly shows that the RGD peptide is well-immobilized onto the polymer film.

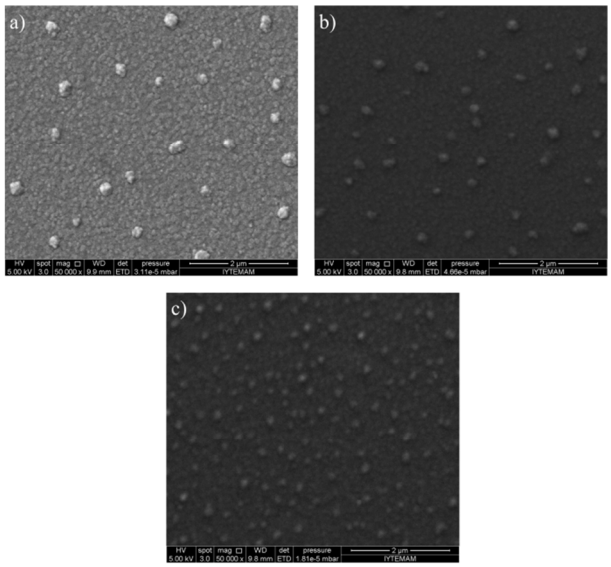

Fig. 4. SEM images of a) ITO, b) ITO/mSNS-NH$_2$ and c) ITO/SNS-mNH$_2$/RGD surfaces (with 50000x magnification).

AFM also supplies the morphological information about surfaces. Fig. 5 shows the characteristic AFM images of the surface topography. The polymer coated surface is fairly smooth according to 2D (Fig. 5a) and 3D (Fig. 5b) images. It is obvious that the immobilization of the RGD peptides brings the heterogeneity of the formed structure on the surface. On the other hand, increased roughness was observed after RGD immobilization at 2D (Fig. 5c) and 3D (Fig. 5d) images. Root mean squares (RMS) of roughness were measured as 1.8 nm and 2.2 nm for the polymer coated and RGD modified surfaces, respectively.

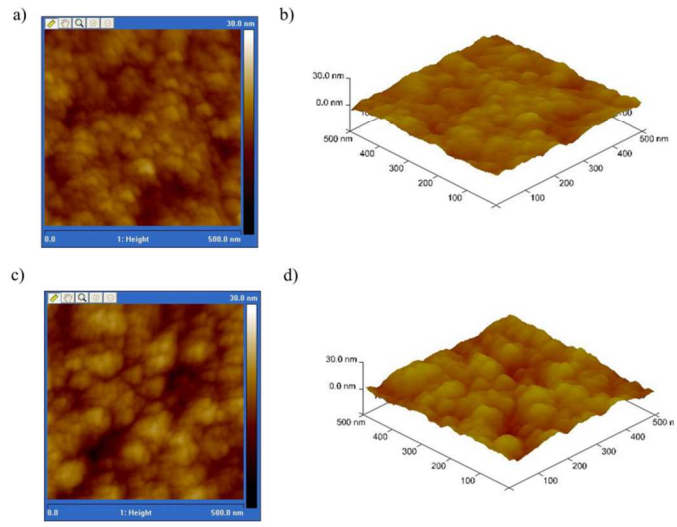

Fig. 5. a) 2D, b) 3D topographic AFM height images of ITO/mSNS-NH_2 and c) 2D, d) 3D topographic AFM height images of ITO/SNS-mNH_2/RGD surfaces.

In terms of increasing surface roughness, AFM and SEM results are consistent with each other. The increase roughness of surfaces has direct effect on cell adhesion and proliferation as cell type dependent manner.[23, 24, 46-48] Therefore, investigation of cellular morphology of different cell lines on surfaces have essential importance.

Cell Culture Studies

Conducting polymer thickness on the surface can be controlled by changing the scan number during electropolymerization.[49] The polymers were deposited on the ITO glass with scans of 5, 10, and 25 cycles. The film thickness of the poly-(SNS-mNH_2) was determined to be 16.0 ± 2.1, 26.0 ± 5.1, 31.0 ± 0.7 nm for 5, 10, and 25 cycles, respectively (n=3). After the modification of each surface, cell adhesion experiments were performed as described in experimental section. The relationship between the average cell number per mm^2 and film thickness was shown in Fig. 6. The 26 nm polymer deposited surface was the best effective substrate for cell adhesion. On the other hand, significantly lower cell adhesion was observed with the 16 nm film thickness. This might be due to less functional amino groups for RGD binding. The 31 nm polymer deposited surface showed non homogenous film formation and some structural defects. Additionally, significantly lower cell adhesion was observed as 16 nm polymer. One possible reason for this, structural deformations on polymer might decrease RGD binding or hindered the right conformation of RGD to interact with the cells. Also, literature reports that the material topography, stiffness, charge and wettability can also affect cell adhesion and proliferation.[50-52] As a result, the modified surface prepared with 26 nm polymer thickness was selected for subsequent experiments.

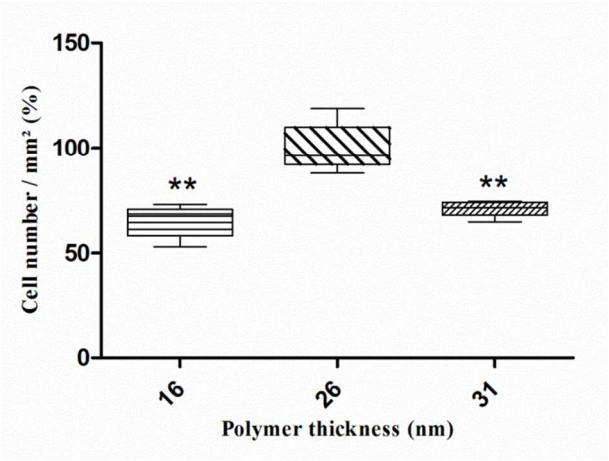

Fig. 6. Effects of film thickness to number of Vero cells after 24 h incubation on RGD functionalized surfaces (n=3). Maximum cell adhesive surface (26 nm thickness) was accepted as 100%.

Time dependent adhesion and proliferation behaviors of Vero cells on the ITO/SNS-mNH_2, ITO/SNS-mNH_2/RGD and commercially used polystyrene (PS) were investigated. Although ITO/SNS-mNH_2 surface showed similar cell adhesion properties at 4, 24 and 48 h, it has been observed that polymer coated surface affected negatively to cell proliferation at 72 h. Because of the cell adhesion to RGD peptides modified surfaces time dependent and increase after initial cell adhesion, higher cell proliferation differences was observed at 72 h. [53] Therefore, RGD modified surface had better cell proliferation after initial cell adhesion than polymer coated and PS surfaces owing to cell adhesive peptide modification (Fig. 7).

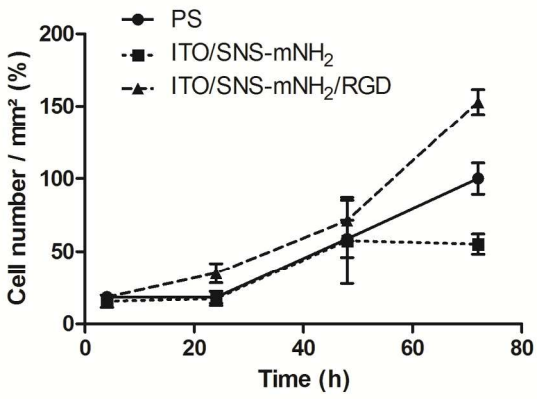

Fig. 7. Time dependent Vero cell adhesion and proliferation on ITO/SNS-mNH_2, ITO/SNS-mNH_2/RGD, and control polystyrene surfaces (n=3).

Vero cell morphology after 72 h incubation on RGD modified surface was examined by AFM. The AFM image of the single layer of fixed and proliferated cells on the modified surface is shown in Fig. S3. On ITO/SNS-mNH_2/RGD surface healthy and well proliferated cells were observed.

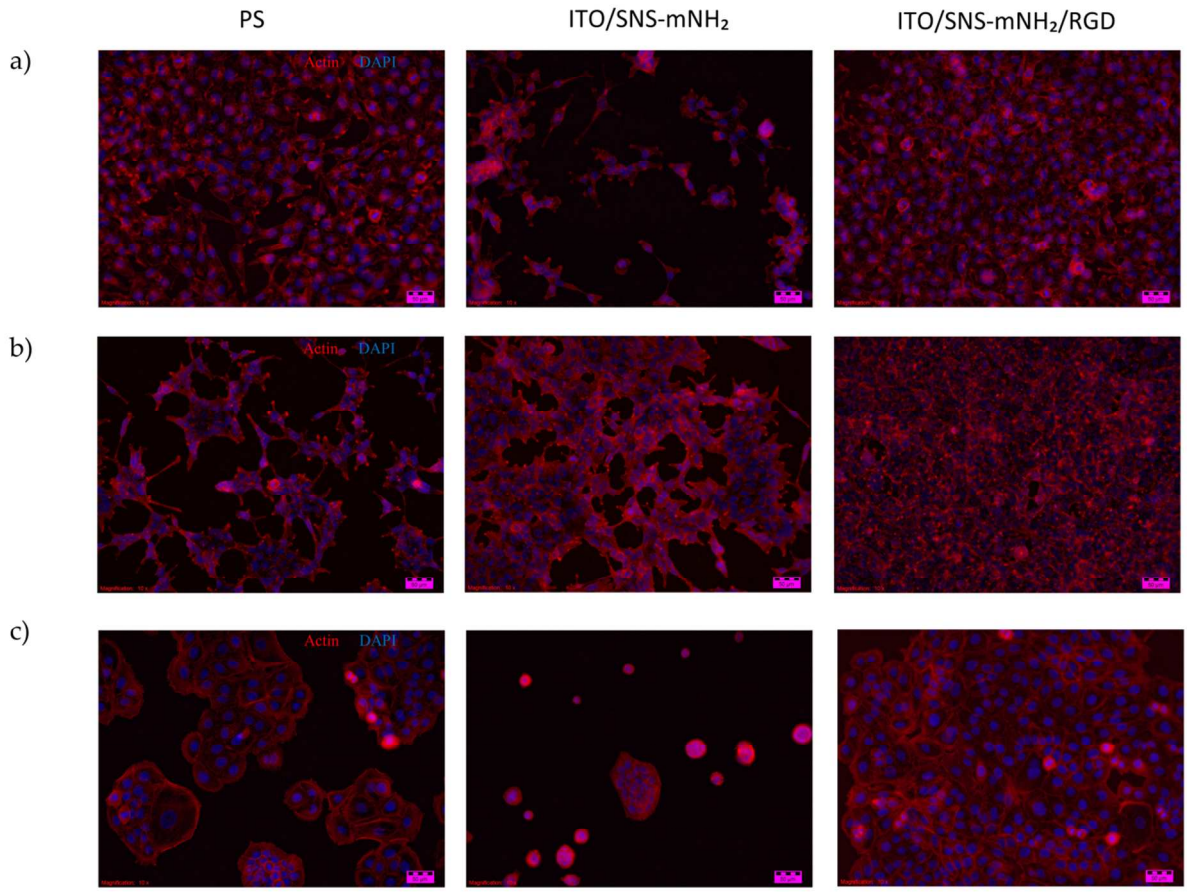

Fig. 8. Proliferation behaviors of a) Vero, b) HaCaT, and c) SH-SY5Y cell lines after 72 h incubation on control polystyrene, ITO/SNS-mNH$_2$, and ITO/SNS-mNH$_2$/RGD surfaces. Actin (Red) and DAPI (blue) staining were performed. Scale bar: 50 µm.

Effects of surface modification on proliferation behaviors of Vero, HaCaT, and SH-SY5Y cell lines were compared. Fig. 8 represents that all of the cell lines attach and spread on the RGD modified surface to a greater extent than the polymer coated surface. Although HaCaT and Vero cell lines could not spread over polymer coated surfaces, an enhancement proliferation of cells was observed on RGD functionalized surfaces. On the other hand, In Fig. 8 SH-SY5Y cell line grows as one top of the other in clusters and extent short neurites out of the clusters without any differentiation due to its characteristic feature.[54] This cell line had maximum proliferation than other cell lines on RGD modified and also polymer modified surfaces due to its highly aggressive characteristics.[55, 56] Proliferation behaviour of this cell line on polymer coated and RGD modified surfaces was further examined by SEM (Fig. S4).

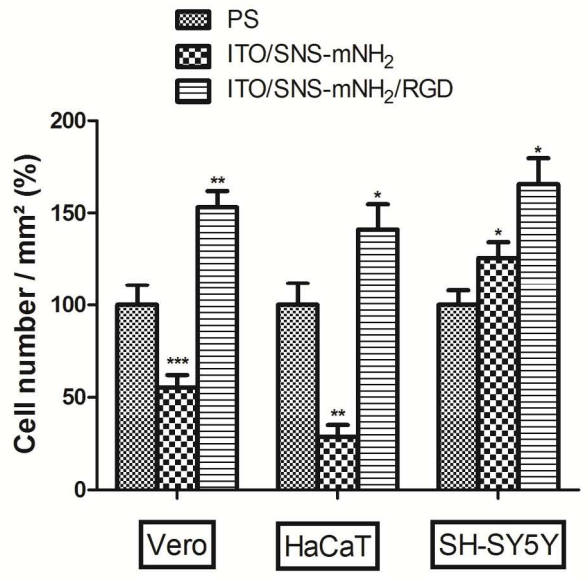

Fig. 9. Number of Vero, HaCaT and SH-SY5Y cell lines after 72 h incubation on control polystyrene, ITO/SNS-mNH$_2$, and ITO/SNS-mNH$_2$/RGD surfaces (n=3). Asterisks indicate the differences compared to PS surface for each cell line.

The relationship between average number of cells per mm^2 and different cell lines were shown in Fig. 9. ITO/SNS-mNH_2/RGD surfaces showed higher cell proliferation for all of the cell lines than control and polymer coated surfaces. The spreading of all cells on the RGD modified surfaces indicate that the cells interact with the RGD motif which was immobilized to the surface of conducting scaffolds. Cells can interact with RGD as integrin dependent manner and start to organize actin fibers to proliferate on surfaces.

Experimental

Materials

ITO coated glasses (24 x 24 mm) were obtained from TEKNOMA, Turkey. The ITO coated glass had sheet resistance of 8 - 10 ohm / sq with and thickness of 150-170 μm.
RGD peptide, EDC (1-Ethyl-3-(3-dimethylaminopropyl) carbodiimide), lithium perchlorate ($LiClO_4$), sodium perchlorate ($NaClO_4$), ethanol, isopropanol, acetone, Triton X-100, formaldehyde (37%), 4, 6-diamino-2-phenylindol (DAPI) purchased from Sigma. Acetonitrile (ACN), phosphate buffered saline (pH 7.4, PBS) was prepared using 8.0 g/L NaCl, 0.2 g/L KCl, 1.44 g/L $Na_2HPO_4.2H_20$ and 0.2 g KH_2PO_4 (Merck).
Dulbecco's modified Eagle Medium (DMEM), DMEM / Ham's F12 mixture (F12), penicillin/streptomycin (P/S) (10000/10000 units) and 200 mM L-Glutamine were purchased from Lonza. Foetal bovine serum (FBS) was purchased from Biowest.
CytoPainter Phalloidin-iFluor 555 reagent was purchased from Abcam.

Apparatus

Voltammetric experiments were carried out with a PalmSens Electrochemical measurement system (Palm Instruments, Houten, The Netherlands), where the modified ITO-glass was used as the working electrode. An Ag^+/AgCl electrode (with 3.0 M KCl saturated with AgCl as the internal solution, Metrohm Analytical, CH-9101) and platinum electrode (Metrohm, Switzerland, www.metrohm.com) were used as reference and counter electrodes, respectively. The electrodes were inserted into a conventional electrochemical cell (10 mL).
Olympus CKX41 model inverted microscope equipped with DC30 camera was used for cellular imaging.
A Keithley electrometer 2400 was used two probe measurements. Electrical contacts were made using silver paste. AFM analyses were performed by Veeco MultiMode V AS-130 (''J'') model for surface characterization. Philips XL-30S FEG model SEM was used. Contact angle measurements performed by Attension Theta. All reported data were given as the average of three measurements ±SD.

Synthesis of 3-(2,5-di(thiophen-2-yl)-1H-pyrrol-1-yl)aniline

A modified procedure for the synthesis of SNS-mNH_2, 3-(2,5-di(thiophen-2-yl)-1H-pyrrol-1-yl)aniline has been established. The polymer was synthesized from 1,4-di(2-thienyl)-1,4-butanedione and benzene-1,3-diamine in the presence of catalytical amount of propionic acid. A round-bottomed flask equipped with an argon inlet and magnetic stirrer was charged with 1,4-di(2-thienyl)-1,4-butanedione (0.35 M), benzene-1,3-diamine (0.45 M), propionic acid (0.36 M) and toluene. The resultant mixture was stirred and refluxed for 24 h under argon. Evaporation of the toluene, followed by flash column chromatography (SiO_2 column, elution with dichloromethane), afforded the desired compound.

Construction of biofunctional surface

Initially, the ITO glasses were cleaned with sequential sonication in acetone, isopropyl alcohol, ethanol and distilled water. Electrochemical polymerization of monomer was potentiodynamically carried out between the potential range -+0.5 V and +1.2 V (versus Ag^+/AgCl) in 0.1 M $NaClO_4$ / $LiClO_4$ / ACN medium at a scan rate of 0.1 V s^{-1}. The polymer coated surface was washed with distilled water to remove unbound residues. The presence of the free amine groups on the conducting polymer backbone can be utilized for the covalent attachment of RGD peptides *via* formation of amide bonds. Thus, EDC reaction was used to immobilize RGD peptide onto the conducting polymer coated surface. To activate carboxyl groups of the RGD peptide, RGD (0.05 mg/mL) and 0.2 M EDC were dissolved in pH 7.4 PBS buffer and incubated at 1200 rpm for 15 min. Then, polymer coated surface was incubated with activated RGD peptide during overnight. ITO-glasses were rinsed with PBS and distilled water three times to remove unbound molecules.
Surfaces electrochemically characterized by CV and DPV. CV of poly-(SNS-mNH_2) on ITO-glass carried out between the potential range -0.5 V and +1.2 V (versus Ag^+/AgCl) in 0.1 M $NaClO_4$ / $LiClO_4$/ ACN medium at different scan rates. DPV studies of ITO, ITO/SNS-mNH_2 and ITO/SNS-mNH_2/RGD surfaces were performed between +0.5 V and -0.3 V in 0.1 M KCl and 5.0 mM $K_4Fe(CN)_6$/100 mM PBS.
Film thickness is determined by using cyclic voltammograms in the electropolymerization process. The charge of polymer is calculated from the area of voltammogram and thickness as a ratio of charge is calculated as previously reported.[14, 57]
The experiments were conducted at ambient temperature (25°C).

Cell culture

Vero and HaCaT cell lines were purchased from ATCC and CLS, respectively. Both of the cell lines were maintained in DMEM supplemented with 10% FBS (Biowest), 1.0% P/S, and 2.0 mM L-Glutamine at 37°C in a humidified incubator with 5.0% CO_2 in air. SH-SY5Y (ATCC) maintained in 1:1 mixture of DMEM/F12 supplemented with 10% FBS, and 1.0% P/S at 37°C in a humidified incubator with 5.0% CO_2 in air. All cells were subcultured at 80% confluency by trypsinization every two or three days.
In all experiments, 5×10^1 cell per mm^2 was seeded onto the sterilized surfaces under common cell culture conditions.

Modified ITOs were placed in 6-well plates to maintain cell culture medium.

Polymer thickness effect on Vero cell adhesion was investigated during 24 h. To determine time dependent adhesion and proliferation behaviors of Vero cells, cells were incubated at 37°C for different incubation times (4, 24, 48 and 72 h) on surfaces. Also Vero, HaCaT and SH-SY5Y cells were cultured during 72 h to compare their proliferation behaviors on surfaces. The conventional PS surface was used as control for each experiment. Subsequently, cells were fixed, stained and visualized by FM as described in the sequential section.

Imaging

To determine number of cells on surfaces, cells were fixed with 4.0% formaldehyde in PBS for 1 h at 37°C after different incubation times. Permeabilization of cells was facilitated by treatment with 0.1% Triton X-100 for 4 min. Then, DAPI nucleus staining was performed for 5 min. Cell number was determined at three different locations for each sample by using NIH Image J software. Three different experiments were performed for each condition.

CytoPainter Phalloidin-iFluor 555 Reagent was used to stain F-actin filaments of cells on surfaces. For F-actin staining, cells were fixed with 4.0% formaldehyde in PBS for 30 min. Permeabilization procedure described above was followed by actin staining for 60 min. After extensive washing with PBS, the cells were imaged using a fluorescent microscope with appropriate filters (with 10x magnification).

For SEM and AFM analyses cells were incubated 72 h and fixed on surfaces with 4.0% formaldehyde in PBS for 1 h at 37°C and then air dried during 24 h.[58] AFM was used in tapping mode and SEM analyses carried out at 5.0 kV for all experiments.

The experiments were conducted at ambient temperature (25°C) unless stated otherwise.

Statistical Analysis

GraphPad Prism version 5.03 (GraphPad Software, San Diego, CA) was used to obtain graphs and for statistical analyses. Non-parametric Mann-Whitney U test was used to compare relative cell numbers per surface area among different surfaces. [59] Statistical significance was denoted with *, **, and *** for $p \leq 0.05$, $p \leq 0.01$, and $p \leq 0.001$, respectively.

Conclusions

Here we describe that the electrochemically polymerized SNS-mNH_2 performs well as an immobilization matrix for RGD facilitated cell adhesion. The constructed biofunctional platform is appropriate for optical measurements. Owing to high conductivity, it is also possible to use the proposed surface in electrochemical platforms. The RGD modified surface is cost effective and easily prepared. Therefore, the modified surface can be combined with lab-on-a chip systems to monitor living cell, effects of drugs and chemicals as well as analyzing cellular dynamics *via* optical detection, electrochemical detection or systems that using both.

Acknowledgements

This project was supported by Scientific and Technological Research Council of Turkey (TUBITAK, project number 113Z918) and Ege University Research Foundation (Project numbers; 12-TIP-104 and 14-FEN-023).

METU Central Laboratory is acknowledged for the contact angle and AFM analyses. Also, we thank to IYTE MAM for SEM analyses. The authors also thank to Prof. Dr. S. Sakarya (Adnan Menderes University) and Prof. Dr. H. O. Sercan (Dokuz Eylul University) for their support.

Notes and references

[a]Ege University, Graduate School of Natural and Applied Sciences, Biotechnology Dept., 35100-Bornova/Izmir, Turkey.

[b]Ege University, Institute on Drug Abuse, Toxicology and Pharmaceutical Science, 35100-Bornova/Izmir, Turkey.

[c]Pamukkale University, Faculty of Arts and Science, Chemistry Dept., Denizli, Turkey.

[d]Ege University, Faculty of Science, Biochemistry Dept., 35100-Bornova/Izmir, Turkey.

[e]Ege University, Faculty of Medicine, Psychiatry Dept., 35100-Bornova/Izmir, Turkey.

†Electronic Supplementary Information (ESI) available: See DOI:10.1039/b000000x/

1. E. Primiceri, M. S. Chiriacò, R. Rinaldi and G. Maruccio, *Lab on a Chip*, 2013, **13**, 3789-3802.
2. H. Andersson and A. van den Berg, *Sensors and Actuators B: Chemical*, 2003, **92**, 315-325.
3. K. Gupta, D.-H. Kim, D. Ellison, C. Smith, A. Kundu, J. Tuan, K.-Y. Suh and A. Levchenko, *Lab on a Chip*, 2010, **10**, 2019-2031.
4. P. R. Bidez, S. Li, A. G. MacDiarmid, E. C. Venancio, Y. Wei and P. I. Lelkes, *Journal of Biomaterials Science, Polymer Edition*, 2006, **17**, 199-212.
5. R. A. D'Sa, P. J. Dickinson, J. Raj, B. K. Pierscionek and B. J. Meenan, *Soft Matter*, 2011, **7**, 608-617.
6. J. Yang, D. H. Kim, J. L. Hendricks, M. Leach, R. Northey and D. C. Martin, *Acta Biomaterialia*, 2005, **1**, 125-136.
7. B. Demir, M. Seleci, D. Ag, S. Cevik, E. E. Yalcinkaya, D. O. Demirkol, U. Anik and S. Timur, *RSC Advances*, 2013, **3**, 7513-7519.
8. S. Demirci, F. B. Emre, F. Ekiz, F. Oğuzkaya, S. Timur, C. Tanyeli and L. Toppare, *Analyst*, 2012, **137**, 4254-4261.
9. N. K. Guimard, N. Gomez and C. E. Schmidt, *Progress in Polymer Science*, 2007, **32**, 876-921.
10. R. Ravichandran, S. Sundarrajan, J. R. Venugopal, S. Mukherjee and S. Ramakrishna, *Journal of the Royal Society, Interface / the Royal Society*, 2010, **7 Suppl 5**, S559-579.
11. J. G. Hardy, J. Y. Lee and C. E. Schmidt, *Current opinion in biotechnology*, 2013, **24**, 847-854.
12. A. Gelmi, M. K. Ljunggren, M. Rafat and E. W. H. Jager, *Journal of Materials Chemistry B*, 2014, **2**, 3860-3867.
13. H. Azak, E. Guler, U. Can, D. O. Demirkol, H. B. Yildiz, O. Talaz and S. Timur, *RSC Advances*, 2013, **3**, 19582-19590.
14. F. E. Kanik, E. Rende, S. Timur and L. Toppare, *Journal of Materials Chemistry*, 2012, **22**, 22517-22525.
15. A. B. Sanghvi, K. P. H. Miller, A. M. Belcher and C. E. Schmidt, *Nat Mater*, 2005, **4**, 496-502.
16. B. Seven, M. Bourourou, K. Elouarzaki, J. F. Constant, C. Gondran, M. Holzinger, S. Cosnier and S. Timur, *Electrochemistry Communications*, 2013, **37**, 36-39.
17. J. Wang and M. Jiang, *Langmuir*, 2000, **16**, 2269-2274.

18. F. Ekiz, F. Oguzkaya, M. Akin, S. Timur, C. Tanyeli and L. Toppare, *Journal of Materials Chemistry*, 2011, **21**, 12337-12343.
19. S. Demirci, F. B. Emre, F. Ekiz, F. Oguzkaya, S. Timur, C. Tanyeli and L. Toppare, *Analyst*, 2012, **137**, 4254-4261.
20. E. Sackmann and A.-S. Smith, *Soft Matter*, 2014, **10**, 1644-1659.
21. J. Y. Wong, R. Langer and D. E. Ingber, *Proceedings of the National Academy of Sciences*, 1994, **91**, 3201-3204.
22. B. J. Papenburg, E. D. Rodrigues, M. Wessling and D. Stamatialis, *Soft Matter*, 2010, **6**, 4377-4388.
23. H.-I. Chang and Y. Wang, *Regenerative Medicine and Tissue Engineering—Cells and Biomaterials, InTech: Rijeka, Croatia*, 2011, 569-588.
24. B. Joddar and Y. Ito, *Journal of Materials Chemistry*, 2011, **21**, 13737-13755.
25. G. Delaittre, A. M. Greiner, T. Pauloehrl, M. Bastmeyer and C. Barner-Kowollik, *Soft Matter*, 2012, **8**, 7323-7347.
26. M. Mrksich, *Chem. Soc. Rev.*, 2000, **29**, 267-273.
27. S. P. Low, K. A. Williams, L. T. Canham and N. H. Voelcker, *Biomaterials*, 2006, **27**, 4538-4546.
28. U. Geißler, U. Hempel, C. Wolf, D. Scharnweber, H. Worch and K. W. Wenzel, *Journal of Biomedical Materials Research*, 2000, **51**, 752-760.
29. D. Liu, C. A. Che Abdullah, R. P. Sear and J. L. Keddie, *Soft Matter*, 2010, **6**, 5408-5416.
30. C. Werner, T. Pompe and K. Salchert, in *Polymers for Regenerative Medicine*, Springer, 2006, pp. 63-93.
31. S. E. D'Souza, M. H. Ginsberg and E. F. Plow, *Trends in biochemical sciences*, 1991, **16**, 246-250.
32. G. B. Fields, J. L. Lauer, Y. Dori, P. Forns, Y. C. Yu and M. Tirrell, *Biopolymers - Peptide Science Section*, 1998, **47**, 143-151.
33. D. J. Iuliano, S. S. Saavedra and G. A. Truskey, *Journal of Biomedical Materials Research*, 1993, **27**, 1103-1113.
34. U. Hersel, C. Dahmen and H. Kessler, *Biomaterials*, 2003, **24**, 4385-4415.
35. E. Yildiz, P. Camurlu, C. Tanyeli, I. Akhmedov and L. Toppare, *Journal of Electroanalytical Chemistry*, 2008, **612**, 247-256.
36. G.-B. Lee, H.-C. Wu, P.-F. Yang and J. D. Mai, *Lab on a Chip*, 2014, **14**, 2837-2843.
37. Y.-S. Hsiao, C.-W. Kuo and P. Chen, *Advanced Functional Materials*, 2013, **23**, 4649-4656.
38. D. Bogojevic, M. D. Chamberlain, I. Barbulovic-Nad and A. R. Wheeler, *Lab on a Chip*, 2012, **12**, 627-634.
39. J. H. An, J.-S. Lee, J.-R. Chun, B.-K. Oh, M. D. A. Kafi and J.-W. Choi, *Journal of Nanoscience and Nanotechnology*, 2012, **12**, 5143-5148.
40. Y. Lin, X. Lu, X. Gao, H. Cheng, T. Ohsaka and L. Mao, *Electroanalysis*, 2013, **25**, 1010-1016.
41. G. T. Hermanson, *Bioconjugate techniques*, Academic press, 2013.
42. M. Ak, A. Durmus and L. Toppare, *J Appl Electrochem*, 2007, **37**, 729-735.
43. B. Lu, S. Zhen, S. Zhang, J. Xu and G. Zhao, *Polymer Chemistry*, 2014, **5**, 4896-4908.
44. P. Yang, J. Xie and W. Yang, *Macromolecular Rapid Communications*, 2006, **27**, 418-423.
45. S. Kant, S. Kalia and A. Kumar, *Journal of Alloys and Compounds*, 2013, **578**, 249-256.
46. T. W. Chung, D. Z. Liu, S. Y. Wang and S. S. Wang, *Biomaterials*, 2003, **24**, 4655-4661.
47. L. De Bartolo, M. Rende, S. Morelli, G. Giusi, S. Salerno, A. Piscioneri, A. Gordano, A. Di Vito, M. Canonaco and E. Drioli, *Journal of Membrane Science*, 2008, **325**, 139-149.
48. C. Luo, L. Li, J. Li, G. Yang, S. Ding, W. Zhi, J. Weng and S. Zhou, *Journal of Materials Chemistry*, 2012, **22**, 15654-15664.
49. E. Guler, H. C. Soyleyici, D. O. Demirkol, M. Ak and S. Timur, *Materials Science and Engineering: C*, 2014, **40**, 148-156.
50. J. I. Rosales-Leal, M. A. Rodríguez-Valverde, G. Mazzaglia, P. J. Ramón-Torregrosa, L. Díaz-Rodríguez, O. García-Martínez, M. Vallecillo-Capilla, C. Ruiz and M. A. Cabrerizo-Vílchez, *Colloids and Surfaces A: Physicochemical and Engineering Aspects*, 2010, **365**, 222-229.
51. H. B. Wang, M. Dembo and Y. L. Wang, *American journal of physiology. Cell physiology*, 2000, **279**, C1345-1350.
52. Y. Yang, K. Kulangara, R. T. S. Lam, R. Dharmawan and K. W. Leong, *ACS Nano*, 2012, **6**, 8591-8598.
53. D. L. Hern and J. A. Hubbell, *J Biomed Mater Res*, 1998, **39**, 266-276.
54. J. Kovalevich and D. Langford, *Methods in molecular biology (Clifton, N.J.)*, 2013, **1078**, 9-21.
55. J. Do, I. Kim, J. Lee and D.-K. Choi, *BioChip J*, 2011, **5**, 165-174.
56. L. Zhang, H. Liang, W. Cao, R. Xu and X. L. Ju, *Brazilian Journal of Medical and Biological Research*, 2014, **47**, 548-553.
57. M. Kesik, F. E. Kanik, G. Hızalan, D. Kozanoglu, E. N. Esenturk, S. Timur and L. Toppare, *Polymer*, 2013, **54**, 4463-4471.
58. M. J. Doktycz, C. J. Sullivan, P. R. Hoyt, D. A. Pelletier, S. Wu and D. P. Allison, *Ultramicroscopy*, 2003, **97**, 209-216.
59. P. E. McKnight and J. Najab, in *The Corsini Encyclopedia of Psychology*, John Wiley & Sons, Inc., 2010.

